ELSEVIER

J. Non-Newtonian Fluid Mech. 86 (1999) 229–252

Journal of Non-Newtonian Fluid Mechanics

# Non-linear flows in porous media

Shijie Liu*, Jacob H. Masliyah[1]

*Department of Chemical and Materials Engineering, University of Alberta, Edmonton, Alta., Canada T6G 2G6*

Received 20 March 1998; received in revised form 12 September 1998

**Abstract**

A volume averaging approach is applied to derive governing equations for purely viscous homogeneous flows in porous media. Additional terms appear in the volume averaged governing equations related to porosity, tortuosity, shear factor, dispersion coefficient and macroscopic viscosity. Flow in porous media is non-linear in nature in that the shear factor, the dispersion coefficient and the macroscopic viscosity are functions of flow velocity. A shear factor model is proposed based on flow through orifice plates and the macroscopic viscosity is defined for purely viscous flows. The predictions of flow velocity profile and pressure drop using the proposed model agree well with published experimental results. © 1999 Elsevier Science B.V. All rights reserved.

*Keywords:* Porous media; Packed beds; Macroscopic viscosity; Orifice; Network model; Volume averaging; Non-Newtonian flow

## 1. Introduction

The mechanism of the flow in porous media involves many problems vital to science and industry. Notable examples are: to name a few, recovery of fuels from underground oil and gas reservoirs; mass and heat transfer operations in packed columns; solid catalyzed reactions; and fate of pollutants in soil. Owing to its complexity and non-linear nature, flow in porous media has been studied, by and large, through direct experimentation.

For a single phase generalized Newtonian fluid flow, the governing partial differential equations are given by the continuity (or conservation of mass) equation

$$\frac{\partial \rho^*}{\partial t} + \nabla^*(\rho^* \vec{v}^*) = 0 \tag{1}$$

* Corresponding author. Tel.: +1-780-492-3321; fax: +1-780-492-2881; e-mail: shijie.liu@ualberta.ca
[1]E-mail: jacob.masliyah@ualberta.ca

0377-0257/99/$ – see front matter 
PII: S0377-0257(98)00210-9

and the (conservation of) momentum equation

$$\frac{\partial(\rho^*\vec{v}^*)}{\partial t} + \nabla^*(\rho^*\vec{v}^*\vec{v}^*) + \nabla^* p^* - \rho^*\vec{g} - \nabla^*\mu^*[(\nabla^*\vec{v}^*) + (\nabla^*\vec{v}^*)^{\mathrm{T}}] = 0, \tag{2}$$

where $\rho^*$ is the density of the fluid; $t$ is time; $\vec{v}^*$is the flow velocity field; $p^*$ is the pressure in the fluid; $\vec{g}^*$ is the gravity vector and $\mu^*$ is the apparent dynamic viscosity of the fluid. The apparent dynamic viscosity can be a function of the flow conditions for non-Newtonian fluids. When the dynamic viscosity is constant (invariant to flow), the fluid is called a Newtonian fluid. In these equations, the superscript * is added for all the variables to distinguish between the quantities that will be involved in this study and those simply expressed in the fluid continuum level: Eqs. (1) and (2). Together, Eqs. (1) and (2) are also termed the Navier–Stokes equations. These equations are valid within a fluid phase.

For flow in porous media, Eqs. (1) and (2) are still valid within the open pores (fluid phase). However, complications arise due to the complicated structure of the pores in a porous medium. It is a formidable task to keep track of all the pores, let alone to solve the flow problem inside these pores together. It is a common practice to treat the porous medium as a continuum medium. Therefore, the fluid flow equations need to be modified to account for the presence of the solid matrix as a continuum in the fluid continuum. There are two continuum media: fluid that is in motion and the solid matrix that is rigid and stationary. The exact governing equations for the fluid flow are expected to be different from Eqs. (1) and (2).

A one-dimensional empirical model for single phase Newtonian fluid flow in porous media was introduced by Darcy [1] based on the unidirectional water permeation in a fountain. When the flow is weak (or at low discharge fluid rates), the pressure drop is linearly related to the flow discharge rate. Darcy's law is expressed as

$$u = -\frac{k}{\mu}\left(\frac{\mathrm{d}p}{\mathrm{d}x} - \rho g_x\right), \tag{3}$$

where $u$ is the superficial fluid flow velocity (or discharge rate), $k$ is the permeability of the porous medium taken as a constant in applications, $\mu$ is the dynamic viscosity of the fluid (Newtonian), $p$ is the pressure, $x$ is the linear coordinate in the direction of flow, $\rho$ is the density of the fluid and $g_x$ is the gravity in the direction of flow. For flow in a packed bed of spheres, the permeability is well characterized by the Kozeny–Carman equation. In Eq. (3), the superscript * is not posed to the variables because the quantities are in an average sense (including the porous medium continuum). Darcy's law has been generalized and used in flow simulations for multidimensional single phase and multiphase flows. In comparison with Eq. (2), Darcy's law lacks the flow diffusion and non-linear effects. Therefore, the utility of Darcy's law is highly restrictive.

For unidirectional flow in a packed bed, the pressure drop is observed to vary with the flow (discharge) rate non-linearly. The well-known Ergun equation can be expressed as

$$-\frac{\mathrm{d}p}{\mathrm{d}x} + \rho g_x = 150\mu\frac{(1-\epsilon)^2}{d_{\mathrm{s}}^2\epsilon^3}u + 1.75\frac{1-\epsilon}{d_{\mathrm{s}}\epsilon^3}\rho u^2, \tag{4}$$

where $\epsilon$ is the porosity of the medium and $d_{\mathrm{s}}$ is the equivalent spherical diameter of the particles that

make up the porous medium matrix. The coefficients (150 and 1.75) are found to vary with porosity and particle shapes. Subsequently, the original Ergun equation has been subject to modifications by a number of researchers, to name a few: MacDonald et al. [2], Comiti and Renaud [3], Liu et al. [4] and Mauret and Renaud [5]. Even the non-linearity expressed by Eq. (4) does not seem to agree with the experimental observations completely [4]. Nevertheless, Eq. (4) is the simplest form of equation for unidirectional flow in packed beds (porous media) that can give a reasonable account of the inertial effects. When the last term on the right-hand side of Eq. (4) is omitted, the equation is better known as the Kozeny–Carman equation. The general form of Eq. (4) is also known as the Darcy–Forchheimer equation.

To remedy the defect in the Darcy's law for the lacking of flow diffusion effects, Brinkman [6] intuitively added a viscous diffusion term into the Darcy's law:

$$-\nabla p + \rho\vec{g} = \frac{\mu}{k}\vec{v} - \hat{\mu}\nabla^2\vec{v}, \tag{5}$$

where $\hat{\mu}$ is the effective viscosity of the fluid flowing in the porous medium and $\vec{v}$ is the superficial flow velocity field. Brinkman [6] further qualified that the effective viscosity should be the same as the dynamic viscosity of the (Newtonian) fluid in order to account for the existing experimental data. Eq. (5) has been widely used (with $\hat{\mu} = \mu$) for weak flow simulations, for example, [6,7]. Recently, Givler and Altobelli [8] found that the effective viscosity is a function of flow rate. Therefore, the viscous diffusion term added by Brinkman [6] still needs quantification/examination. The same extension can be made to Eq. (4) to include the diffusion effect as that Eq. (5) is compared to Eq. (3). By adding the viscous diffusion term to Eq. (4), the resulting equation is known as the Darcy–Brinkman–Forchheimer or Brinkman–Forchheimer equation.

A few investigators have set forth to give some theoretical qualifications to the Darcy's law and the Brinkman's equation. For example, Whitaker [9]; Slattery [10] and Bear [11] have pioneered an approach known as the volume averaging. Heuristic arguments can be provided for the Darcy's law and the Brinkman equation by volume averaging Eq. (2). More terms evolve from the averaging process and need to be accounted for. Liu and Masliyah [12] has also applied volume averaging and attempted to address all the aspects of flow behaviors: inertia and diffusion. Still, there is a need for a better understanding and a unified approach to flow and transport in porous media.

The objectives of this study are (i) to revisit the volume averaging technique and derive at the governing equations based on Eqs. (1) and (2); (ii) to close the extra terms present in the volume averaged equations; (iii) to solve the volume averaged equations and compare the solutions with the existing experimental data in the literature.

## 2. Volume averaging procedure

The representative elementary volume, or REV, is a conceptual space unit. When the probing (measuring) volume is at least of REV, measurable characteristics of the porous medium become continuum quantities. Volume averaging is a technique that makes the measurable quantities continuum properties based on the REV concept. The continuum or macroscopic governing equations are derived based on the microscopic governing equations.

The *volume average* of a quantity for fluid, $\phi$, is the average taken over the entire REV

$$\phi = \frac{1}{V}\int_V \phi^* \, \mathrm{d}V, \tag{6}$$

where $V$ is the volume of the REV and $\phi^*$ is the local (microscopic) quantity. The volume averaged quantity is also known as the superficial quantity.

The *intrinsic phase average* of a quantity, $\phi_\epsilon$, is the average value of a quantity with respect to the fluid only,

$$\phi_\epsilon = \frac{1}{V_\mathrm{i}}\int_{V_\mathrm{i}} \phi^* \, \mathrm{d}V, \tag{7}$$

where $V_\mathrm{i}$ is the volume of the fluid in the REV. The porosity is defined by

$$\epsilon = \frac{V_\mathrm{i}}{V}, \tag{8}$$

which is also a volume averaged quantity. The deviation of a quantity in the fluid phase, $\hat{\phi}$, is the difference between the local value and the phase intrinsic averaged value of that quantity,

$$\hat{\phi} = \phi^* - \phi_\epsilon. \tag{9}$$

Here $\phi$ can be a scalar or a vector. Note that $\hat{\phi}$ is defined only inside the fluid.

Owing to the torturous passages in porous media, the local velocities are higher than otherwise linear (straight line) measurements. The local (interstitial) velocities in the porous medium passages are known to be higher than the simple Dupuit approximation [3–5,13–15]. Therefore, the intrinsic volume averaged flow velocity is given by the following ad hoc expression:

$$\vec{v}_\epsilon = \tau\left(\frac{1}{V_\mathrm{i}}\int_{V_\mathrm{i}} \vec{v}^* \, \mathrm{d}V\right), \tag{10}$$

where $\tau$ is the tortuosity and is defined as

$$\tau = \frac{\mathrm{d}x}{\mathrm{d}x^*}. \tag{11}$$

Here $x^*$ represents the overall microscopic (curved) coordinate and $x$ represents the corresponding macroscopic coordinate. In general, $\tau$ should be a tensor rather than a scalar. In many applications, $\tau$ is also regarded as a transport property, i.e., when different transport quantity is considered different value for $\tau$ is needed. For simplicity, we shall assume $\tau$ to be a scalar (i.e., the porous medium is isotropic) and unique for a given porous medium.

One should note that strictly speaking, Eq. (11) is valid only along the axis of a torturous passage in a porous medium and therefore, Eq. (10) is not a strictly valid volume averaged expression. However, it is a good (phenomenological) model to describe the flow behavior in porous media. This

phenomenological model will also be used from hereon to the volume averaging expressions involving space derivatives and fluxes.

The volume averaged velocity and the intrinsic phase averaged velocity are related by

$$\vec{v} = \epsilon \vec{v}_\epsilon, \tag{12}$$

which is also known as the Dupuit approximation.

Volume averaging of governing equations can be performed by averaging over the REV, term by term. To simplify the volume averaging procedure, one can work out the averaging of the basic blocks of the balance equations. The volume averaged basic blocks are also known as the volume averaging rules. Some of these volume averaging rules are given as follows.

### 2.1. Time derivative rule

$$\frac{1}{V}\int_V \frac{\partial \phi^*}{\partial t}\,\mathrm{d}V = \frac{\partial(\epsilon\phi_\epsilon)}{\partial t}. \tag{13}$$

This rule is an extension to Leibnitz' rule on taking the derivative of an integral with respect to a parameter [16] and differentiating on multiple parts. It is illustrated by the following equation:

$$\frac{\partial(\epsilon\phi_\epsilon)}{\partial t} = \frac{\partial}{\partial t}\left(\frac{1}{V}\int_V \phi^*\,\mathrm{d}V\right) = \frac{1}{V}\int_V \frac{\partial \phi^*}{\partial t}\,\mathrm{d}V + \frac{\partial V}{\partial t}\frac{\partial}{\partial V}\left(\frac{1}{V}\int_V \phi^*\,\mathrm{d}V\right) = \frac{1}{V}\int_V \frac{\partial \phi^*}{\partial t}\,\mathrm{d}V. \tag{14}$$

### 2.2. Gradient rule on a solid surface-vanishing quantity

$$\frac{1}{V}\int_V \nabla^*\phi^*\,\mathrm{d}V = \nabla(\tau\epsilon\phi_\epsilon) + \frac{1}{V}\int_{S_\mathrm{i}} \vec{n}\phi^*\tau\,\mathrm{d}S. \tag{15}$$

where $S_\mathrm{i}$ is the total fluid–solid matrix interface in the REV. This rule is derived primarily for the case where the values of $\phi_\mathrm{i}^*$ are nearly zero on the solid surface, $S_\mathrm{i}$. Therefore, the surface integral term on the right-hand side of Eq. (15) is negligible. However, if $\phi_\mathrm{i}^*$ values are not zero on the solid surface, the surface integral term must be evaluated.

This rule can be obtained by employing the Gauss's theorem. When applying the Gauss's theorem, one should note that the tortuosity needs to be considered. To assist in deriving this rule, Fig. 1 shows a schematic of an REV. Regions (1) and (3) represent the solid matrix and region (2) represents the fluid phase (or voids). The boundary of the REV, $\partial V$, consists of $S_{+\mathrm{i}}$ and $S_{-\mathrm{i}}$. Here $S_{+\mathrm{i}}$ is the fluid portion and $S_{-\mathrm{i}}$ the solid matrix portion of the boundary of the REV. The following is a brief derivation of this rule:

$$\frac{1}{V}\int_V \nabla^*\phi^*\,\mathrm{d}V = \frac{1}{V}\int_{\partial V} \phi^*\vec{n}\tau\,\mathrm{d}S$$

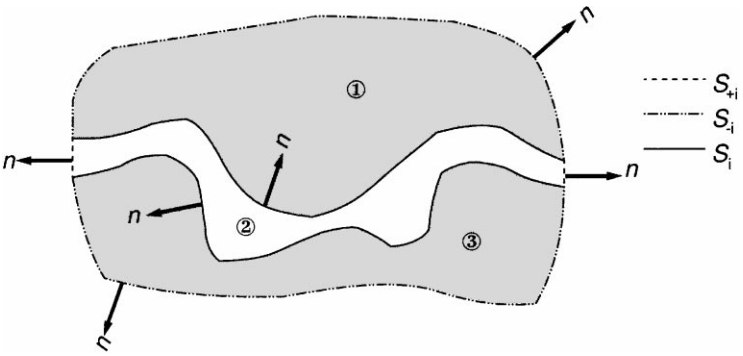


Fig. 1. Planar schematic of an REV containing porous matrix and a fluid phase in region (2).

$$\frac{1}{V}\int_V \nabla^*\phi^*\,\mathrm{d}V = \frac{1}{V}\left[\int_{\partial V}\tau\epsilon\phi_\epsilon\vec{n}\,\mathrm{d}S - \left(\int_{\partial V}\tau\epsilon\phi_\epsilon\vec{n}\,\mathrm{d}S\right) + \int_{\partial(1)}\tau\phi^*\vec{n}_{(1)}\,\mathrm{d}S + \int_{\partial(2)}\tau\phi^*\vec{n}_{(2)}\,\mathrm{d}S + \int_{\partial(3)}\tau\phi^*\vec{n}_{(3)}\,\mathrm{d}S\right]$$

$$\frac{1}{V}\int_V \nabla^*\phi^*\,\mathrm{d}V = \nabla(\tau\epsilon\phi_\epsilon) + \frac{1}{V}\left[-\left(\int_{S_{+\mathrm{i}}}\tau\epsilon\phi_\epsilon\vec{n}\,\mathrm{d}S + \int_{S_{-\mathrm{i}}}\tau\epsilon\phi_\epsilon\vec{n}\,\mathrm{d}S\right) + \int_{S_{+\mathrm{i}}}\tau\phi^*\vec{n}\,\mathrm{d}S + \int_{S_\mathrm{i}}\tau\phi^*\vec{n}\,\mathrm{d}S\right]$$

$$\frac{1}{V}\int_V \nabla^*\phi^*\,\mathrm{d}V = \nabla(\tau\epsilon\phi_\epsilon) + \frac{1}{V}\left[-\left(\int_{S_{+\mathrm{i}}}\tau\phi_\epsilon\vec{n}\,\mathrm{d}S\right) + \int_{S_{+\mathrm{i}}}\tau\phi^*\vec{n}\,\mathrm{d}S + \int_{S_\mathrm{i}}\tau\phi^*\vec{n}_1\,\mathrm{d}S\right]$$

$$\frac{1}{V}\int_V \nabla^*\phi^*\,\mathrm{d}V = \nabla(\tau\epsilon\phi_\epsilon) + \frac{1}{V}\left[\int_{S_\mathrm{i}}\tau\phi^*\vec{n}\,\mathrm{d}S + \int_{S_{+\mathrm{i}}}\tau\hat{\phi}\vec{n}\,\mathrm{d}S\right], \tag{16}$$

where $\partial(1)$ is the surface enclosing region (1) and $\vec{n}_{(1)}$ is the out normal of region (1). Similar notations for regions (2) and (3) are also used. Noting that the region (2) contains the fluid phase, we have $\vec{n}_{(2)} = \vec{n}$. The surface integrals for $\phi_\mathrm{i}^*$ in region (1) and (3) are zero because $\phi^*$ is not defined inside the solid matrix. The final equality of the above equation can be reduced to Eq. (15).

### 2.3. Gradient rule on a non-solid surface–vanishing quantity

$$\frac{1}{V}\int_V \nabla^*\phi^*\,\mathrm{d}V = \tau\epsilon\nabla\phi_\epsilon + \frac{\tau}{V}\int_{S_\mathrm{i}}\vec{n}\hat{\phi}\,\mathrm{d}S. \tag{17}$$

This rule is very much similar to the previous gradient rule, Section 2.2. However, the extra surface integral on the right-hand side is about the deviation not the quantity itself. While the previous rule is specially useful when the quantity itself is nearly zero on the interfaces, this rule is good to the case where the deviation or the gradient of the quantity is nearly zero on the solid surface. A short derivation is given by:

$$\frac{1}{V}\int_V \nabla^*\phi^*\,\mathrm{d}V = \frac{1}{V}\left[\tau\int_{V_\mathrm{i}} \nabla\phi_\epsilon\,\mathrm{d}V + \int_V \nabla^*\phi^*\,\mathrm{d}V - \tau\int_{V_\mathrm{i}} \nabla\phi_\epsilon\,\mathrm{d}V\right]$$

$$\frac{1}{V}\int_V \nabla^*\phi^*\,\mathrm{d}V = \tau\epsilon\nabla\phi_\epsilon + \frac{\tau}{V}\left[\int_{\partial(1)} \phi^*\vec{n}_{(1)}\,\mathrm{d}S + \int_{\partial(2)} \phi^*\vec{n}_{(2)}\,\mathrm{d}S + \int_{\partial(3)} \phi^*\vec{n}_{(3)}\,\mathrm{d}S - \int_{\partial(2)} \phi_\epsilon\vec{n}_{(2)}\,\mathrm{d}S\right]$$

$$\frac{1}{V}\int_V \nabla^*\phi^*\,\mathrm{d}V = \tau\epsilon\nabla\phi_\epsilon + \frac{\tau}{V}\left[0 + \int_{S_{+\mathrm{i}}} (\phi^* - \phi_\epsilon)\vec{n}\,\mathrm{d}S + \int_{S_\mathrm{i}} (\phi^* - \phi_\epsilon)\vec{n}\,\mathrm{d}S + 0\right]$$

$$\frac{1}{V}\int_V \nabla^*\phi^*\,\mathrm{d}V = \tau\epsilon\nabla\phi_\epsilon + \frac{\tau}{V}\left[\int_{S_\mathrm{i}} \hat{\phi}\vec{n}\,\mathrm{d}S + \int_{S_{+\mathrm{i}}} \hat{\phi}\vec{n}\,\mathrm{d}S\right], \tag{18}$$

where the notations follow closely with those of Eq. (16).

### 2.4. Pressure gradient rule

Traditionally, the pressure gradient was not treated differently from other types of gradients. The difference has been brought up by Liu et al. [4]. In averaging the pressure, one must note that the pressure inside the immobile solid material is not defined and is also irrelevant to the flow. The solid matrix can sustain pressure and stresses. The fluid, on the other hand, will transmit the pressure and stresses to adjacent fluid elements or the solid matrix. When stress is applied, the fluid will respond by flow and the solid matrix will deform according to its rigidity. When the solid matrix is immobile, rigid and not supported by the fluid, it will not share the load with the fluid. Body force or gravity results in hydrostatic pressure, thus the gravity term should be treated the same way as the pressure. Therefore, the averaged pressure gradient is given by

$$\frac{1}{V}\int_{V_\mathrm{i}} (\nabla^* p - \rho^*\vec{g})\,\mathrm{d}V = \tau(\nabla p - \rho\vec{g}), \tag{19}$$

where $p$ is short for, $p_\epsilon$, the phase intrinsic averaged pressure. Since the 'volume averaged pressure' is not to be used in this study in any form, this notation will not give rise to any confusion. This rule can be derived similar to rule Section 2.3. However, one should note that the load of the phase under concern will not be shared by the solid matrix.

### 2.5. Divergence rule

Fluxes are commonly encountered in mathematical–physical models. There are two contributions to a flux: diffusion and convection. Let the flux be given by

$$\Gamma^* = \rho^* \vec{v}^* \phi^* - D^* \nabla^* \phi^*, \tag{20}$$

where $D^*$ is the molecular diffusivity (for mass transport) or the fluid viscosity (for momentum transport). The volume averaging on the divergence of a flux is given as

$$\begin{aligned}\frac{1}{V}\int_V \nabla^* \cdot (\rho^* \vec{v}^* \phi^* - D^* \nabla^* \phi^*)\,\mathrm{d}V &= \nabla \cdot \left[\rho \vec{v} \phi_\epsilon - \tau D \left(\frac{1}{V}\int_V \nabla^* \phi^*\,\mathrm{d}V\right)\right] \\ &+ \frac{1}{V}\int_{S_\mathrm{i}} (\rho^* \vec{v}^* \phi^* - D^* \nabla^* \phi^*) \cdot \vec{n}\tau\,\mathrm{d}S + \frac{1}{V}\int_{S_{+\mathrm{i}}} \left[\rho^* \vec{v}^* \phi^* - D^* \nabla^* \phi^* - \frac{1}{V_\mathrm{i}}\int_{V_\mathrm{i}} (\rho^* \vec{v}^* \phi^* - D^* \nabla^* \phi^*)\,\mathrm{d}V\right] \\ &\cdot \vec{n}\tau\,\mathrm{d}S + \nabla \cdot \left\{\frac{\tau}{V}\int_{V_\mathrm{i}} \left[\rho^* \vec{v}^* \phi^* - D^* \nabla^* \phi^* - \rho \frac{\vec{v}}{\tau\epsilon}\phi_\epsilon + D\left(\frac{1}{V_\mathrm{i}}\int_{V_\mathrm{i}} \nabla^* \phi^*\,\mathrm{d}V\right)\right]\mathrm{d}V\right\}.\end{aligned} \tag{21}$$

This rule is obtained by employing the same technique as used in deriving the gradient rules. Volume averaging of the flux, Eq. (20), renders

$$\begin{aligned}\epsilon\Gamma_\epsilon = \frac{1}{V}\int_V (\rho^* \vec{v}^* \phi^* - D^* \nabla^* \phi^*)\,\mathrm{d}V &= \rho \frac{\vec{v}}{\tau}\phi_\epsilon - D\left(\frac{1}{V}\int_V \nabla^* \phi^*\,\mathrm{d}V\right) \\ &+ \frac{1}{V}\int_{V_\mathrm{i}} \left[\rho^* \vec{v}^* \phi^* - D^* \nabla^* \phi^* - \rho \frac{\vec{v}}{\tau\epsilon}\phi_\epsilon + D\left(\frac{1}{V_\mathrm{i}}\int_{V_\mathrm{i}} \nabla^* \phi^*\,\mathrm{d}V\right)\right]\mathrm{d}V.\end{aligned} \tag{22}$$

Similar to Eq. (16), the averaging of the divergence on the flux can be written as

$$\frac{1}{V}\int_V \nabla^* \cdot \Gamma^*\,\mathrm{d}V = \nabla(\tau\epsilon\Gamma_\epsilon) + \frac{1}{V}\left[\int_{S_\mathrm{i}} \tau\Gamma^* \cdot \vec{n}\,\mathrm{d}S + \int_{S_{+\mathrm{i}}} \tau(\Gamma^* - \Gamma_\epsilon) \cdot \vec{n}\,\mathrm{d}S\right]. \tag{23}$$

Substituting Eqs. (20) and (22) into Eq. (23), one can obtain Eq. (21). Since all the terms are kept so far, there are no limitations on the type of fluxes that can apply this rule.

One can identify two main groups of the extra surface/intrinsic volume integral terms for the divergence rule: exchange of the quantity $\phi^*$ inside the fluid phase between the REV and the surrounding, i.e., the interaction within the fluid, and the exchange of the quantity $\phi^*$ between the fluid and the solid matrix, i.e., the interaction of the fluid with the solid matrix. The first surface integral on

the right-hand-side of Eqs. (21) and (23) corresponds to the net flux into the solid matrix. The rest of the extra integrals in these equations represent the interaction within the fluid.

Owing to the imbedded volume averaging of a gradient in the divergence rule and the difference in the averaging of the gradient, one can have two different final forms for Eq. (21).

## 3. Closures

Closures are important in modeling of flow and transport in porous media. Even the familiar case of the fluid continuum, take for example, the diffusion can be regarded as a closure for accounting the effect of the molecular Brownian motion on the spreading of molecules. Closures are normally called to evaluate the complicated interaction groups difficult to obtain otherwise. A closure for the interaction within the fluid, i.e., the surface and intrinsic phase volume integral terms of Eq. (21), should give rise to 'diffusion'. Using this similarity, one can postulate that

$$\begin{aligned}
&\frac{1}{V}\int_{S_{+\mathrm{i}}}\left[\rho^*\vec{v}^*\phi^* - D^*\nabla^*\phi^* - \frac{1}{V_\mathrm{i}}\int_{V_\mathrm{i}}\rho^*\vec{v}^*\phi^* - D^*\nabla^*\phi^*)\mathrm{d}V\right]\cdot\vec{n}\tau\,\mathrm{d}S \\
&\quad + \nabla\cdot\left\{\frac{\tau}{V}\int_{V_\mathrm{i}}\left[\rho^*\vec{v}^*\phi^* - D^*\nabla^*\phi^* - \frac{\vec{v}}{\tau\epsilon}\rho\phi_\epsilon + D\left(\frac{1}{V_\mathrm{i}}\int_{V_\mathrm{i}}\nabla^*\phi^*\,\mathrm{d}V\right)\right]\mathrm{d}V\right\} \\
&= -\nabla\cdot[\tau\epsilon\underline{\underline{K}}\cdot\nabla(\rho\phi_\epsilon)],
\end{aligned} \tag{24}$$

where $\underline{\underline{K}}$ is the dispersion coefficient tensor. For the case of constant $D^*$, the dispersion coefficient is linearly related to the norm of the mass flow velocity when the convection is dominated. The total flux of $\phi^*$ into the solid matrix can be closed by

$$\frac{1}{V}\int_{S_\mathrm{i}}\left(\vec{n}\cdot\vec{v}^*\rho^*\phi^* - D^*\frac{\partial\phi^*}{\partial n}\right)\tau\,\mathrm{d}S = \tau DF\left(\frac{\rho|\vec{v}|}{\epsilon D}\right)\tau\epsilon(\phi_\epsilon - \phi_\mathrm{s}), \tag{25}$$

where $F(\cdot)$ is the interaction coefficient between the fluid and the solid matrix, $\phi_\mathrm{s}$ is the averaged value of $\phi$ at the fluid–solid interface. $F$ is also termed the shear factor. Similar form has been used, by among others Du Plessis [17].

The tortuosity for an unconsolidated media (packed beds) is given by

$$\tau = \epsilon^{1/2}. \tag{26}$$

The above equation is known as the Bruggemann equation.

The dispersion coefficient tensor is known to be of the following form:

$$\underline{\underline{K}} = d_\mathrm{s}|\vec{v}|D_\mathrm{T}\begin{bmatrix}\delta_\mathrm{L} & 0 & 0\\ 0 & 1 & 0\\ 0 & 0 & 1\end{bmatrix}, \tag{27}$$

where $D_T$ is the transverse dispersion coefficient and $\delta_L$ is the normalized longitudinal dispersion factor. For packed beds of spheres, Liu [18] gave

$$D_T = 10.7\epsilon^{11/3}(1-\epsilon)^{2/3}, \tag{28}$$

$$\delta_L = 30, \tag{29}$$

where $\delta_L$ is valid for low Reynolds number flows: Re < 10 for gas flow and Re < 1000 for liquid flows. At high Reynolds numbers, $D_T$ remains the same. However, $\delta_L$ is reduced to 4.

The macroscopic viscosity for a Newtonian fluid is the same as the dynamic viscosity of the fluid. For non-Newtonian fluid flows, the macroscopic viscosity is expected to be different from the dynamic viscosity of the fluid. The macroscopic viscosity is the intrinsic volume average of the dynamic viscosity. Owing to the complex structure of the porous matrix and the local shear conditions, the macroscopic viscosity needs to be determined by experimentation or modeling. Liu and Masliyah [19] proposed a treatment for the macroscopic viscosity. For a Cross fluid, the dynamic viscosity is characterized by

$$\mu^* = \mu^*_\infty + \frac{\mu^*_0 - \mu^*_\infty}{1 + \left(|\underline{\underline{\dot{\gamma}}}^*|/\dot{\gamma}_c\right)^m}, \tag{30}$$

where $\underline{\underline{\dot{\gamma}}}^*$ is the microscopic shear rate (or deformation) tensor; $\dot{\gamma}_c$ is the critical shear rate at which the apparent dynamic viscosity is the average between the low and the high shear viscosities; and $m$ is the power-law index. The subscript 0 stands for low shear and $\infty$ for high shear. Since non-Newtonian fluids are commonly mixtures of macromolecules in a solvent. It is thus natural to consider the macromolecule–solid surface interactions as well in defining the macroscopic viscosity. Corresponding to Eq. (30), the macroscopic viscosity for the Cross fluid flow in a packed bed of spheres is given by

$$\mu = \mu_\infty + \frac{\mu_0 - \mu_\infty}{1 + (\delta_W^4 + \mu_R\mu_W(1-\delta_W^4))/(\delta_W^4 + \mu_W(1-\delta_W^4))k_2/(k_2+m)(R_v k_3 \delta_W)^m}, \tag{31}$$

where

$$\mu_0 = \frac{\mu^*_0}{\delta_W^4 + \mu_W(1-\delta_W^4)}, \tag{32}$$

$$\mu_\infty = \frac{\mu^*_\infty}{\delta_W^4 + \mu_R\mu_W(1-\delta_W^4)}, \tag{33}$$

$$R_v = \frac{3|\vec{v}|}{\epsilon^{10/3} d_s \dot{\gamma}_c}, \tag{34}$$

$$\mu_R = \frac{\mu^*_\infty}{\mu^*_0}, \tag{35}$$

$$\mu_W = \frac{\mu^*_0}{\mu^*_f + (\mu^*_0 - \mu^*_f)\mu_{WR}}, \tag{36}$$

$$\mu_{\mathrm{WR}} = \frac{\mu^*_{\mathrm{L0}} - \mu^*_{\mathrm{f}}}{\mu^*_0 - \mu^*_{\mathrm{f}}}, \tag{37}$$

$$\delta_{\mathrm{W}} = \max\left[1 - \frac{3(1-\epsilon)\delta_{\mathrm{d}}}{\epsilon d_{\mathrm{s}}},\, 0\right], \tag{38}$$

$$k_2 = 1 + \frac{6}{k_1/3} = 1 + 36\epsilon^{7/6}(1-\epsilon), \tag{39}$$

$$k_3 = \frac{1}{\pi} + 1.16\epsilon^{7/12}(1-\epsilon)^{1/2}, \tag{40}$$

$$k_1 = \frac{1}{2\epsilon^{7/6}(1-\epsilon)}. \tag{41}$$

$\delta_{\mathrm{d}}$ is the thickness of the layer of fluid near the solid surface, in which the fluid viscosity is $\mu^*_{\mathrm{L0}}$. The fluid is assumed of a mixture of macromolecules and a solvent fluid. The viscosity of the solvent fluid is $\mu^*_{\mathrm{f}}$.

The shear factor for single fluid flow has been modeled by: among others, Du Plessis [17]; Liu et al. [4] and Liu and Masliyah [12]. A new shear factor model will be proposed later in this study. Therefore, at this point, we shall leave this section.

## 4. Volume averaged Navier–Stokes equations

For simplicity, we consider here the fluids to be purely viscous, i.e., a generalized Newtonian fluid, and the fluid density is constant, i.e., incompressible flow. When no porous medium is present, or the porosity is exactly unity, the flow is governed by the Navier–Stokes equations. They are also referred to as the continuity (conservation of mass) and momentum (conservation of momentum) equations. These equations have been given as Eqs. (1) and (2).

The volume averaged governing flow equations are obtained by averaging the Navier–Stokes equations in an REV. The volume averaged continuity equation is obtained by applying the time derivative rule and the divergence rule on Eq. (1), noting that $D^* \equiv 0$ and $\phi^*$ is the fluid phase identity function ($\phi^* = 1$ inside the fluid and $\phi^* = 0$ inside the solid matrix). Setting $\phi_\epsilon = 1$, one obtains

$$\epsilon\frac{\partial \rho}{\partial t} + \nabla(\rho\vec{v}) = 0. \tag{42}$$

One can observe that the volume averaged continuity equation is very similar to the original continuity Eq. (1).

The volume averaged momentum equation can be obtained by applying the time derivative rule, pressure gradient rule and the divergence rule together with the gradient rule on a solid surface–vanishing quantity. In this case, $\phi^* = \vec{v}^*$, $\phi_\epsilon = \vec{v}/\tau\epsilon$, $\phi_\epsilon = \vec{v}/\tau$. As the flow velocity vanishes on the solid surface, the gradient rule a solid surface–vanishing quantity is appropriate for the gradient of the

velocity vector. The final volume averaged equation can be arranged to give

$$\frac{\partial}{\partial t}\frac{\rho\vec{v}}{\tau}+\nabla\cdot\left(\frac{\rho\vec{v}\vec{v}}{\epsilon\tau}\right)+\tau(\nabla p-\rho\vec{g})-\nabla\cdot\tau\mu[(\nabla\vec{v})+(\nabla\vec{v})^{\mathrm{T}}]-\nabla\cdot\left(\tau\epsilon\underline{\underline{K}}\cdot\nabla\frac{\rho\vec{v}}{\tau\epsilon}\right)+\tau\mu F\vec{v}=0. \tag{43}$$

Eqs. (42) and (43) are the volume averaged Navier–Stokes equations for homogeneous fluid flow in isotropic porous media.

For steady Newtonian fluid flow in a porous medium of constant porosity, Eq. (43) can be reduced to the Brinkman's equation by neglecting the inertial terms. Furthermore, when the viscous and dispersion terms are neglected, Eq. (43) can be reduced to the Darcy's law.

## 5. A new shear factor model

The flow straits in the packed bed or porous medium can be considered as a network of passages. A two-dimensional schematic representation of the flow straits is shown in Fig. 2. The flow path ways are interconnected and the passages are short. The flow straits can be interpreted as consisting of mixing cells and the short connecting passages between the mixing cells. In a two-dimensional setting, there are three connecting passages extending out from each mixing cell as one can observe more clearly from the regional blowup on the right in Fig. 2. The short passages may be regarded as orifices having a diameter of $d_o$ and a length of $\delta$. Therefore, the flow straights may be regarded as flow through a network of orifices. In a three-dimensional setting, there will be five connecting passages extending out from one mixing cell. Each orifice represents one free direction of flow. Therefore, the network model built in such a manner represents a free space blocked from one side by a solid wall at each unit cell (mixing cell).

Let the length to diameter ratio of the connecting pores be $s_\Phi$,

$$s_\Phi=\frac{\delta}{d_o}. \tag{44}$$

The pressure drop for flow through each orifice has been studied recently by Liu et al. [20]. They found that the pressure drop can be described by the following equation:

$$\frac{-\Delta p}{2\mu u}d_o=9+16s_\Phi+0.45\frac{\mathrm{Re}_o^2}{4C_o^2+\mathrm{Re}_o^2}(\mathrm{Re}_o-C_o), \tag{45}$$

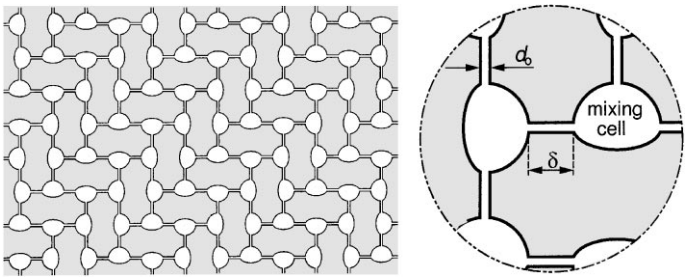


Fig. 2. Network of flow straits formed by mixing cells and connecting pores in a two-dimensional setting.

where $u$ is the discharge flow velocity through the orifice; $\mathrm{Re_o}$ is the orifice Reynolds number and $C_o$ is the transitional parameter, $C_o = 8$. The orifice Reynolds number, $\mathrm{Re_o}$, is defined as

$$\mathrm{Re_o} = \frac{d_o \rho u}{\mu}. \tag{46}$$

Eq. (45) can be adopted to estimate the pressure drop for unidirectional flow in packed beds. Therefore, one can find a shear factor model based on Eq. (45). The procedure for this conversion is given by Liu and Masliyah [12].

Before we proceed in converting Eq. (45) directly to the shear factor, let us discuss the proper definition of Reynolds number for flow in packed beds and porous media. There are a number of definitions for the flow Reynolds number in porous media/packed beds. However, none of these definitions are valid for both low porosity, $\epsilon < 0.4$, and high porosity, $\epsilon \to 1$, media. Rather than the traditional approach of defining the Reynolds number based on the flow rate, we hereby redefine the Reynolds number based on the fully-developed pressure drop for creeping flow through a passage. It is given by

$$\mathrm{Re} = 24 \frac{\text{Kinetic Energy of Flow}}{(\text{Channel Diameter}) \times (\text{Pressure Drop per Unit Channel Length})}$$

$$\mathrm{Re} = 24 \left[ \frac{\rho u_e^2/(2d_e)}{-\Delta p/(L/\tau)} \right]_{\text{creeping flow}} = \frac{3}{4k_1} \frac{d_e \rho u_e}{\mu}, \tag{47}$$

where $d_e$ is the equivalent hydraulic passage diameter, $d_e = 4 \times$ void volume/solid surface area, and $k_1$ is the first shape factor of the passage, for a circular duct, $k_1 = 2$. The numerical constants are added simply for the convenience of expressing the final equation. It is clear that the definition given by Eq. (47) differs from the traditional definition for flow in a duct just by a numerical constant: 3/8 for a circular duct. For flow through a packed bed, the shape factor $k_1$ is defined by Eq. (41). Using the equivalent passage diameter defined by Liu et al. [4], Eq. (47) can be reduced to

$$\mathrm{Re} = \epsilon \frac{d_s \rho |\vec{v}|}{\mu}. \tag{48}$$

Here, $d_s$ is the equivalent spherical particle diameter of the packed particles. Clearly, the Reynolds number defined by Eq. (48) has a definitive value for the entire range of the porosity $\epsilon$. Therefore, this definition is preferred over other existing definitions which normally has a factor of $1/(1-\epsilon)$ explicitly appearing in the expressions.

Eq. (45) is valid for an orifice whose pore is straight. It is expected that the pores in porous media are curved [4]. Using the approach given by Liu et al. [4], one can combine the orifice pressure drop model with that for a curved passage. A shear factor model can thus be obtained based on a combination of the flow through orifices and flow in curved ducts, which is given as

$$F = F_o \left[ 0.637 + \frac{0.363}{s_\Phi} + 0.048 \frac{1 + a_c s_\Phi (1 - \epsilon^{1/2})^{1/2}}{s_\Phi} \frac{\mathrm{Re}^2}{4C^2 + \mathrm{Re}^2} (\mathrm{Re} - C) \right], \tag{49}$$

where $F_0$ is the shear factor under very weak flow conditions; $a_c$ is curvature effect factor; $C$ is the transitional parameter; and the coefficients are all obtained from the orifice pressure drop Eq. (45). For

packed beds (especially packed beds of spheres), $s_\Phi$ is usually around unity (Dybbs and Edwards [21]). The viscous term coefficients: 0.637 and 0.363, come from 16 and 9, respectively. The overall numerical value of the viscous term at $s_\Phi = 1$ has been normalized to unity, in order to render these values. The inertial constant: 0.0484, is obtained by noting the difference between the definitions of Reynolds number, Eqs. (46) and (48), together with the normalization utilized for the viscous term, that is, $0.45 \times (8/3)(1/(9+16))$. The same procedure can be used to define the transitional parameter, $C$, from $C_o$. It is given by

$$C = C_o \times \frac{3}{8} = 3. \tag{50}$$

The parameters $F_o$ is given [12] by

$$F_o = \frac{18(1-\epsilon)}{\epsilon^{29/6} d_s^2}. \tag{51}$$

The only parameter that still needs to be defined for Eq. (49) is the curvature effect factor, $a_c$. We have not used the packed bed pressure drop data directly up to this point. To evaluate the curvature effect factor, we shall make use of the inertial constant found in the existing correlations. Since most of the packed beds of spheres have a porosity near 0.4, we assume that the inertial term is accounted correctly by the Ergun equation at $\varepsilon = 0.4$. Using this information, we obtain

$$a_c = 0.46. \tag{52}$$

Therefore, the complete shear factor based on the orifice network is reduced to

$$F = \frac{18(1-\epsilon)}{\epsilon^{29/6} d_s^2}\left[0.637 + \frac{0.363}{s_\Phi} + 0.048\frac{1 + 0.46 s_\Phi (1-\epsilon^{1/2})^{1/2}}{s_\Phi}\frac{\mathrm{Re}^2}{36+\mathrm{Re}^2}(\mathrm{Re}-3)\right], \tag{53}$$

where we retain $s_\Phi$ as an additional shape factor for the packed bed/porous medium. For packed beds of spheres, $s_\Phi \approx 1$. For packed beds of particles having very different shapes, the value of $s_\Phi$ is expected to differ from unity.

## 6. Flow in packed beds

Packed columns are commonly utilized for unit mass transfer operations such as distillation and absorption. They are also used as fixed bed reactors. In these applications, the column is a circular cylinder. For simplicity, we consider here only the fully-developed single phase flows in such a column. The flow is expected to be axisymmetrical. In this case, only one non-zero volume averaged velocity component exist: the axial flow velocity. Therefore, the governing equation for a generalized Newtonian fluid, Eq. (43), is reduced to a single ordinary differential equation given by

$$\mu F u - \frac{1}{r\tau}\frac{\mathrm{d}}{\mathrm{d}r}\left(r\tau\epsilon K_{rr}\frac{\mathrm{d}}{\mathrm{d}r}\frac{\rho u}{\tau\epsilon} + r\tau\mu\frac{\mathrm{d}u}{\mathrm{d}r}\right) = -\frac{\mathrm{d}p}{\mathrm{d}x}, \tag{54}$$

where $K_{rr}$ is the transverse (radial) dispersion coefficient and $u$ is the axial ($x$-) velocity component. The

boundary conditions for Eq. (54) are the no-slip wall conditions. Together with the boundary conditions and known porosity profile, Eq. (54) can be used to solve for the pressure drop with a given flow rate or solve for the velocity distribution with a given pressure drop or flow rate.

For a packed tower or fixed bed, there is a marked difference between the solid matrix structure near the containing wall and that in the bulk. This difference is better described by a porosity variation. For the first few particle thickness near the bounding wall, the volume averaged porosity is higher than that in the bulk, which can render higher portion of the fluid to pass through this region. This behavior has been well characterized by among others, Vortmeyer and Schuster [22], Vafai [23], Hunt and Tien [24], Liu and Masliyah [12,25]. When annular averaging is performed with a rather small band in the radial direction, one can also observe a fluctuation in the fluid flux near the wall region. This behavior is due to the porosity variation in the near wall region. While normally the spatial oscillation is considered to be removed when volume averaging is applied, there are cases where the spatial oscillation may be important [26]. Therefore, it is necessary to treat the porosity variations in the near wall region. Previously, Vortmeyer and Schuster [22] utilized an exponential function and Liu and Masliyah [12,25] used a quadratic function to capture the porosity decay from the containing wall for the first one particle region. Kufner and Hofmann [27] applied an exponential decay and cosinusoidal oscillation function to capture both the porosity decay and oscillations. Mueller [28] characterized the porosity decay and oscillation through a Bessel function. One should note that both the exponential decay and the Bessel function decay/oscillation are purely empirical. For simplicity, we prefer the exponential decay and cosinusoidal oscillation concept of [27]. Maintaining the exponential decaying cosinusoidal function, we found a better fit to the experimental data for packed beds of uniform spheres and cylinders as

$$\epsilon = \epsilon_b + (1-\epsilon_b)\mathrm{Er}\left[(1-0.3p_d)\cos\left(\frac{2\pi}{1+1.6\mathrm{Er}^2}\frac{D/2-r}{p_d d_s}\right)+0.3p_d\right], \tag{55}$$

where $D$ is the diameter of the column; $\epsilon_b$ is the porosity in the bulk region; $p_d$ is the period of oscillation normalized by $d_s$ and Er is an exponential decaying function. The exponential decaying function is given by

$$\mathrm{Er} = \exp\left[-1.2p_d\left(\frac{D/2-r}{d_s}\right)^{3/4}\right]. \tag{56}$$

For packed bed of uniform spheres, the period of oscillation is found to be 0.94 sphere diameter, i.e.,

$$p_d = 0.94. \tag{57}$$

For packed bed of uniform cylinders with equal diameter and height, $d$, the particle diameter $d_s$ should be replaced by $d$. The period of oscillation is increased over that for packed bed of uniform spheres due to the geometrical arrangement. It is expected that the period of the oscillation is proportional to the horizontal length one individual particle can stretch statistically. Assuming equal chances of orientation for particles to contact horizontally, vertically and diagonally, the period of oscillation becomes,

$$p_d = 0.94\frac{\sqrt{2}+2}{3} \tag{58}$$

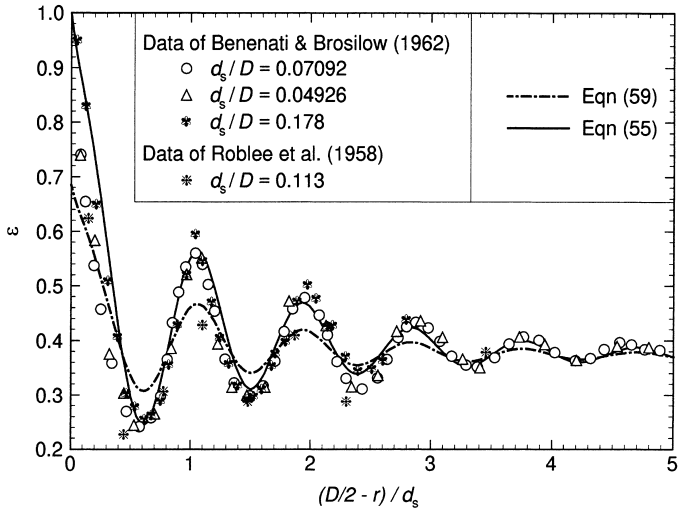


Fig. 3. Porosity variation in the radial direction near the column wall for packed beds of uniform spheres.

Fig. 3 shows the variation of porosity with radial distance from the column wall. The experimental data are taken from [29,30] and the solid curve is drawn with Eq. (55). Here the bulk porosity $\epsilon_b$ is taken to be 0.37. One can observe that Eq. (55) characterizes the oscillation and decay quite well. There are also experimental data available on the packed beds of cylinders. Fig. 4 shows the variation of porosity near the column wall for packed beds of cylinders. The experimental data are taken from [30] and the solid curve is drawn also using Eq. (55) with $\epsilon_b = 0.25$. One can observe that the agreement between the data and the equation is very good. Since cylinders and spheres are common overall shapes random packings, we expect the utility of Eq. (55) in characterizing packed beds.

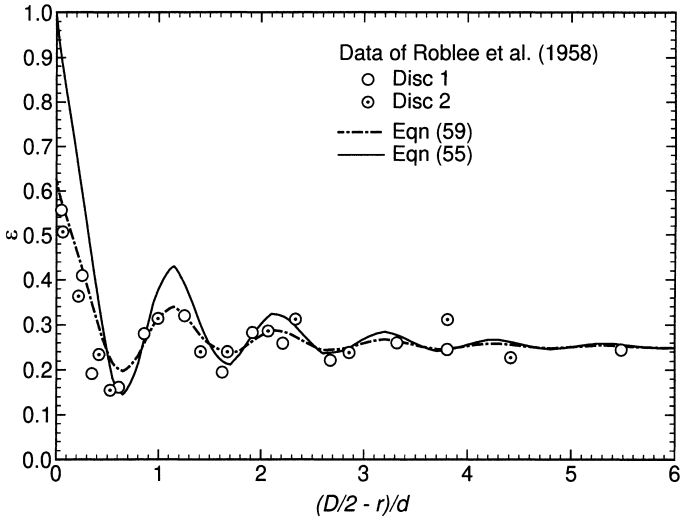


Fig. 4. Porosity variation for packed beds of uniform cylinders whose heights are equal to diameters.

The capture of porosity variation/oscillation by Eq. (55) can lend a means for capturing the flow profile variations/oscillations in the wall region. However, there is no known set of governing equations for flow can be used in association with Eq. (55). We have either the original Navier–Stokes equation which requires no averaging performed or the volume averaged Eq. (54). Eq. (55) implies partial averaging. Utilization of the fully averaged Eq. (54) implies that the variations/oscillations at the length scale of about or less than the particle diameter should be filtered out. On the other hand, Eq. (55) is intended to fully capture the porosity variation/oscillation in the particle size scale. The discrepancy between the requirement of using Eq. (54) and the nature of Eq. (55) forbids a direct combination of these two equations. Direct combination of these equations will lead to incorrect results, especially the pressure drop. To reduce the discrepancy, one needs to modify both equations. Liu and Masliyah [12,25] has noted this discrepancy and devised a treatment for the case where the oscillation has been filtered out. Similar treatment can be used in this case where both the short scale porosity variation and oscillation are retained.

The level of oscillation/variation given by Eq. (55) should be reduced for use with the volume averaged equations. In other words, some averaging for the porosity in the radial direction should be made as well. When all the short range variations/oscillations are filtered out, the porosity becomes that of the bulk porosity. A compromise approach is to take the average between the fully averaged porosity and the locally averaged porosity. To this end, we modify Eq. (55) to give

$$\epsilon = \epsilon_b + \frac{1-\epsilon_b}{2}\mathrm{Er}\left[(1-0.3p_d)\cos\left(\frac{2\pi}{1+1.6\mathrm{Er}^2}\frac{D/2-r}{p_d d_s}\right)+0.3p_d\right], \tag{59}$$

for use with the volume averaged equations. Taking half of the porosity variation/oscillation out is consistent with [12,25]. Eq. (59) is also plotted in Figs. 3 and 4. One can observe that some averaging has been done to the experimental data if one uses Eq. (59) to represent them. Eq. (59) has smoothed out some short range variations. When the average bed porosity is known, Eq. (59) can be integrated to find the bulk porosity, $\epsilon_b$.

For the shear factor as that defined by Eq. (53), there are two parts: the viscous term and the inertial term,

$$F = F_o(d_s, \epsilon) + F_I(d_s, \epsilon, |\vec{v}|). \tag{60}$$

When computing the viscous part, the porosity should be replaced by the average between the bulk porosity, $\epsilon_b$, and the porosity calculated by Eq. (59). There are no changes in the inertial term. Therefore, the shear factor to be used with Eq. (54) should be modified as

$$F = F_o\left(d_s, \frac{\epsilon+\epsilon_b}{2}\right) + F_I(d_s, \epsilon, u), \tag{61}$$

where $\epsilon$ is calculated using Eq. (59).

For the dispersion coefficient, $K_{rr}$, it is normally a function of porosity, particle diameter and the flow velocity. From Eq. (27), we have

$$K_{rr} = 10.7\epsilon^{11/3}(1-\epsilon)^{2/3}d_s u. \tag{62}$$

Since the dispersion is a result of the spatial velocity fluctuations, implementing the detailed porosity change will reduce/eliminate the apparent dispersion to be associated with the volume averaged

equations. Close to the wall, the velocity fluctuation is nearly accounted for when the porosity variation Eq. (59) is utilized. Actually, the wall conditions are treated exactly when the no-slip condition is imposed. There is no velocity fluctuation and dispersion on the column wall to be accounted for. Therefore, for use with Eq. (54) we propose to modify the dispersion coefficient to

$$K_{\mathrm{rr}} = 10.7\epsilon^{11/3}(1-\epsilon)^{2/3} d_{\mathrm{s}} u(1-\mathrm{Er}), \tag{63}$$

where Er is the exponential decay function as defined by Eq. (56).

The fully developed flow behavior in a packed bed can be described by Eq. (54) together with Eqs. (59),(61) and (63). This description will be able to predict the flow velocity variations in the wall region as well as the extra pressure drop due to the presence of the wall.

## 7. Numerical solutions

The numerical solutions for selected cases will be presented here. The governing equation shall be the reduced volume averaged Navier–Stokes Eq. (54). The governing parameters are defined by Eqs. (59),(61) and (63). Owing to the exponential decay and cosinusoidal oscillation of porosity described by Eq. (59), one needs to have fine grid spacing especially for the few particle diameters near the column wall. A uniform grid together with a central difference scheme is used to carry out the numerical analysis.

Eq. (54) is non-linear in $u$ even for a Newtonian fluid flow because both $K_{\mathrm{rr}}$ and $F$ are functions of the flow velocity, $u$. Therefore, the solution can only be obtained by an iterative method. We shall follow the solution procedure of [12,25]. The shear factor term can be linearized at each iteration by Newton's method:

$$Fu = \left(F + \frac{\partial F}{\partial u} u_*\right) u - \frac{\partial F}{\partial u} u_*^2, \tag{64}$$

where $u_*$ stands for the initial guess on $u$ at each iteration and both $F$ and $\partial F/\partial u$ on the right-hand side are evaluated using $u_*$. At each iteration, $K_{\mathrm{rr}}$ can be evaluated based on the initial guess, $u_*$, as well. Thus, the equation can be treated as linear at each iteration. For the first iteration, a flat profile on $u_*$, i.e., $u_* = 1$ everywhere, should suffice. For the subsequent iterations, $u_*$ is replaced every time by the solution of $u$ from the immediate previous iteration. The iteration is repeated until the relative changes of the pressure drop and the velocity are less than a set tolerance. In this study, the tolerance is set at $10^{-6}$.

For simplicity and clarity in presentation, the pressure drop is normalized in the following fashion:

$$F_{\mathrm{P}} = \frac{-\mathrm{d}p/\mathrm{d}x}{\mu_{\mathrm{f}} q(18(1-\epsilon_{\mathrm{av}}))/d_{\mathrm{s}}^2 \epsilon_{\mathrm{av}}^{29/6}}, \tag{65}$$

where $\epsilon_{\mathrm{av}}$ is the average porosity in the column; $q$ is the average superficial axial flow velocity and $\mu_{\mathrm{f}}$ is a reference viscosity. For Newtonian fluid, $\mu_{\mathrm{f}}$ is the same as the dynamic viscosity of the fluid. For polymer solutions or suspensions that exhibit non-Newtonian behaviors, $\mu_{\mathrm{f}}$ is the dynamic viscosity of the solvent. When no confusion may arise, the average bed porosity, $\epsilon_{\mathrm{av}}$, will be denoted as $\epsilon$ hereafter.

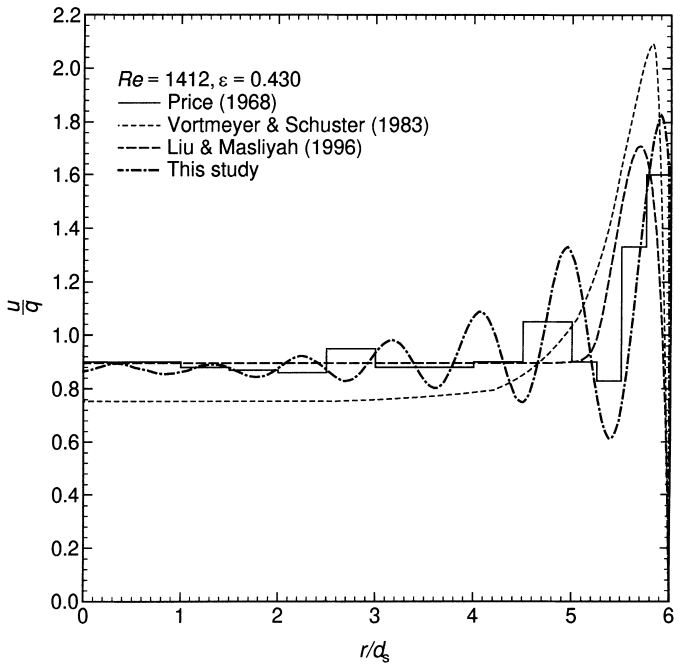


Fig. 5. Axial velocity distribution for air flow through a packed bed of spheres having a column to particle diameter ratio of 12.

The axial velocity profile will be presented by normalizing the superficial velocity with the average discharge flow velocity through the column.

When the flow is uniform, i.e., there are no bounding wall effects and all the velocity gradients are zero, the normalized pressure drop factor, $F_P$, can be obtained by substituting Eqs. (54) and (55) into Eq. (65)

$$F_P = 0.637 + \frac{0.363}{s_\Phi} + 0.048\,\frac{1 + 0.46 s_\Phi (1-\epsilon^{1/2})^{1/2}}{s_\Phi}\,\frac{\mathrm{Re}^2}{4C^2 + \mathrm{Re}^2}\,(\mathrm{Re} - C), \tag{66}$$

where $\epsilon$ is the average bed porosity and Re is the flow Reynolds number based on the average flow velocity and average bed porosity.

Fig. 5 shows the axial velocity profile for air flow through a packed bed of spheres with a sphere to column diameter ratio, $d_s/D$, of 1/12 and an average bed porosity of 0.430 at Re = 1412 based on the average porosity. The porosity hereafter will be used to refer to the average bed porosity, not to confuse with the variable porosity used in the governing differential equations. The bulk porosity, $\epsilon_b$, is 0.4. The normalized pressure drop factor, $F_P$, for this case is found to be 90.4 compared to the uniform flow model, i.e., using Eq. (66), of 86.9. One can observe that the computed velocity profile (dot-dashed curve) represents the experimental data of Price [31] quite reasonable. For comparison, the predictions by Liu and Masliyah [12,25] and Vortmeyer and Schuster [22] are also shown in Fig. 5.

To show how reliable the numerical solution is, Table 1 shows the normalized pressure drop factor, $F_P$, in variation with the number of grid points per particle diameter. One can observe that 1000 grid points per particle is good enough in this case. The need for a large number of grid points per particle is

Table 1
Normalized pressure drop factor in variation with number of grid points

| | | | | | | | |
|---|---|---|---|---|---|---|---|
| Number of grid points per particle | 30 | 50 | 80 | 100 | 150 | 300 | 500 |
| $F_P$ | 93.69 | 92.92 | 92.37 | 92.14 | 91.78 | 91.30 | 91.03 |
| Number of grid points per particle | 1000 | 1500 | 2000 | 3000 | 5000 | 6000 | 10 000 |
| $F_P$ | 90.71 | 90.63 | 90.57 | 90.48 | 90.42 | 90.46 | 90.6 |

due to the sharp change of porosity, especially for the first particle region near the column wall. However, when too many grid points are used, the accumulative computation error will be more significant than the accuracy of the discritization. The computation is made on a Pentium MMX 233 MHz machine. For the highest number of grid points, 10 000 grid points per particle or 60 000 grid points in total, it takes close to half an hour to drive the relative error to $10^{-6}$. For 6000 grid points per particle, it takes about 7.5 min to complete. For 5000 grid points per particle, it takes only 1 min and 12 s to complete. Thus, the solution is relatively easy even for the very fine grid spacings used.

Fig. 6 shows the axial flow velocity profile for an air flow through the packed bed of spheres with $d_s = 4.5$ mm; $D = 20$ mm and $\epsilon = 0.4167$. The experimental data are taken from [27]. The average flow discharge velocity, $q$, is 1.883 m s$^{-1}$ and the average flow Reynolds number, Re, is 2285. Despite the small column size, $2d_s/D = 0.45$, the numerical solution agrees with the experimental data reasonably well. In this case, the pressure drop factor is computed as $F_P = 148.8$. Using the uniform flow model or Eq. (66), however, the pressure drop factor is calculated as 140.5.

We have shown so far that the proposed method computes the flow solutions quite well for Newtonian fluid flows through packed beds. It is desired to be able to compute the flow solutions for non-Newtonian fluid flows as well. To test if the proposed method also works for non-Newtonian fluid

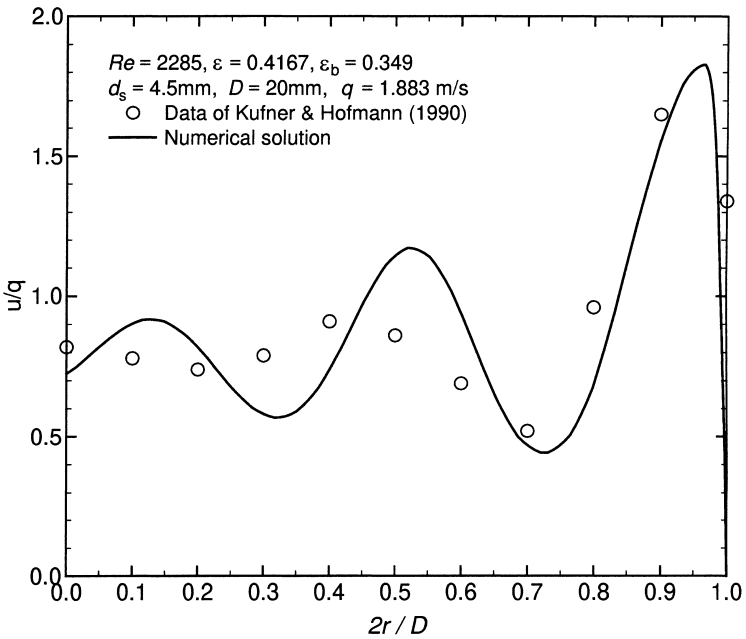


Fig. 6. Axial flow velocity distribution for flow through a packed bed with a particle to column diameter ratio of 0.225.

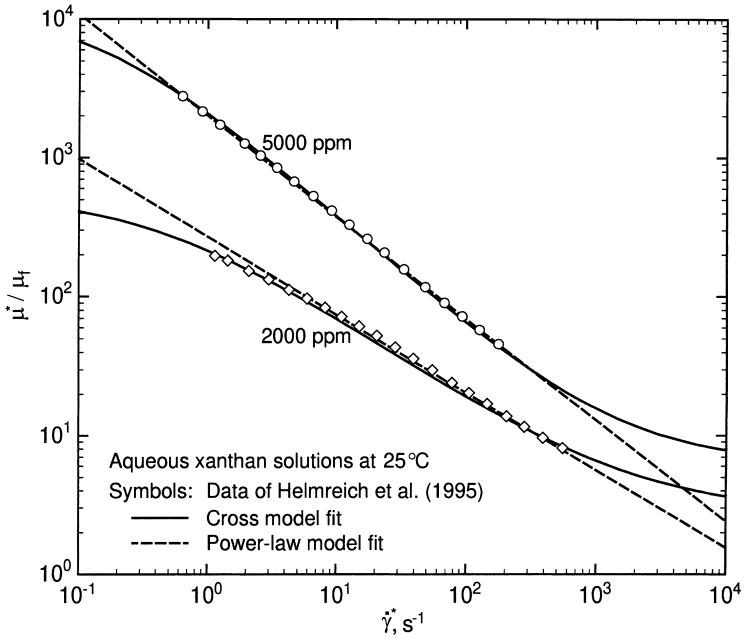


Fig. 7. Rheograms of two aqueous xanthan in water solutions at 25°C.

flows through packed beds, we selected a set of recently published experiments by Helmreich et al. [32]. The rheograms of the non-Newtonian fluids are shown in Fig. 7. The fluids are xanthan gum in water solutions at different xanthan gum concentrations. All the experiments are taken at 25°C, at which the properties of the solvent fluid, water, are given by $\rho^* = 997.0\,\mathrm{kg\,m^{-3}}$ and $\mu_f^* = 0.8897 \times 10^{-3}\,\mathrm{Pa\,s}$. The apparent viscosities of the two solutions can be well represented by the Cross model

$$\frac{\mu^*}{\mu_f^*} = 2.8 + \frac{560}{1 + (\dot{\gamma}^*/0.46\,\mathrm{s^{-1}})^{0.65}} \tag{67}$$

for the 2000 ppm xanthan solution. And,

$$\frac{\mu^*}{\mu_f^*} = 6.4 + \frac{12000}{1 + (\dot{\gamma}^*/0.144\,\mathrm{s^{-1}})^{0.81}} \tag{68}$$

for the 5000 ppm xanthan solution.

The two xanthan solutions were passed through a packed bed of spheres: $d_s = 0.375$ mm; $D = 5$ mm and the average bed porosity of 0.36. The bulk porosity is computed as 0.3294. The normalized pressure drops are shown in Fig. 8. The numerical solutions are obtained in the same manner as those for the Newtonian fluid flows except that the macroscopic viscosity is a function of the local flow velocity and the porosity. The macroscopic viscosity is defined by Eq. (31) and no macromolecule (xanthan molecule)–solid surface interactions are imposed, i.e., $\delta_W = 1$. The numerical solution is found to be just as robust as for the Newtonian fluid flows. One can observe from Fig. 8 that the numerical solutions agree with the experimental data well.

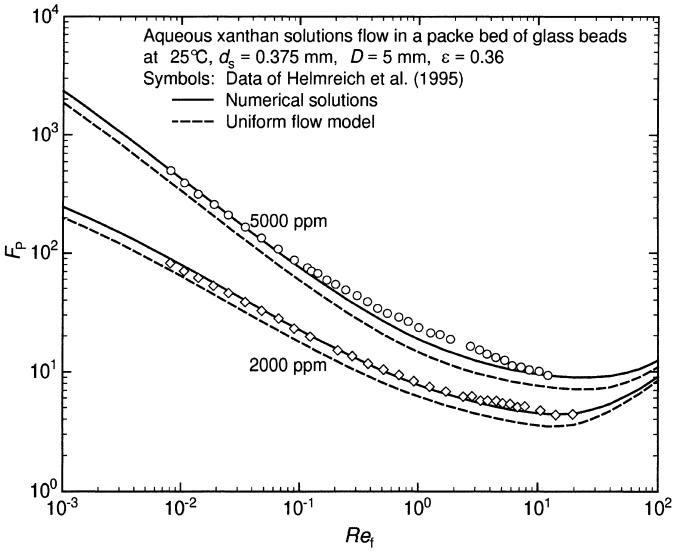


Fig. 8. Pressure drop factor, $F_p$, variation with flow Reynolds number for two xanthan in water solutions (non-Newtonian fluids) of different concentrations.

Fig. 9 shows the axial flow velocity profiles for the three different average flow Reynolds numbers, $Re_f$, for the 2000 ppm aqueous xanthan solution. Here, $Re_f$ is defined by Eq. (48) with the viscosity being the solvent fluid viscosity. One can observe that lower Reynolds number gives rise to higher wall flow. The overall velocity profiles are very similar to those in Figs. 5 and 6.

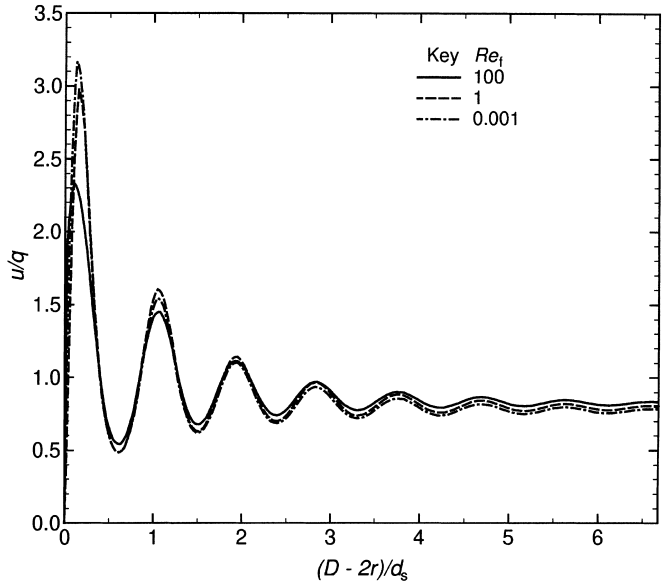


Fig. 9. Axial velocity profiles for the 2000 ppm xanthan in water solution flow through a packed bed of spheres: $d_s/D = 0.075$ and $\epsilon = 0.36$.

In this section, we have shown that the flow behaviors can be solved robustly for both Newtonian and non-Newtonian (generalized Newtonian) fluids flows in packed beds. The predictions agree well with the existing experimental data.

## 8. Conclusions

The governing equations for flow through porous media are derived by volume averaging the Navier–Stokes equations. Additional parameters appearing before the equations are: tortuosity, porosity, macroscopic viscosity, dispersion coefficient and the shear factor. One can find references to all these parameters, however, the combination is unique in this study. The porosity is the voidage of the porous medium and the tortuosity can be defined by the Bruggemann equation for packed beds. The macroscopic viscosity is the same as the fluid viscosity for a Newtonian fluid flow. For a generalized Newtonian fluid flow, the macroscopic viscosity is defined by Liu and Masliyah [19]. The dispersion coefficient is defined by Liu and Masliyah [12] and Liu [18]. A shear factor model is proposed based on the network of orifice plates.

Numerical solutions and procedures are presented in this study for flow through packed beds. The local porosity variation near the column wall is fully implemented and the computed pressure drops and flow velocity profiles agree well with available experimental data for both Newtonian and non-Newtonian (generalized Newtonian) fluids. The numerical solution is robust using the current procedure.

## Acknowledgements

The authors are indebted to the Natural Sciences and Engineering Research Council of Canada (NSERC) and the NSERC Oil Sands Chair for financial support.

## References

[1] H.P.G. Darcy, Flow of Homogeneous Fluids Through Porous Media (M. Muskat Trans.), McGraw-Hill, New York, 1937 (original work published in 1856).
[2] I.F. MacDonald, M.S. El-Sayed, K. Mow, F.A.L. Dullien, Flow through porous media – the Ergun equation revisited, Ind. Eng. Chem. Fund. 18 (1979) 199–208.
[3] J. Comiti, M. Renaud, A new model for determining mean structure parameters of fixed beds from pressure drop measurements: application to beds packed with parallelepipedal particles, Chem. Eng. Sci. 44 (1989) 1539–1545.
[4] S. Liu, A. Afacan, J.H. Masliyah, Laminar flow through porous media, Chem. Eng. Sci. 49 (1994) 3565–3586.
[5] E. Mauret, M. Renaud, Transport phenomena in multi-particle systems – II. Proposed new model based on flow around submerged objects for sphere and fiber beds – transition between the capillary and particulate representations, Chem. Eng. Sci. 52 (1997) 1819–1834.
[6] H.C. Brinkman, A calculation of the viscous force exerted by a flowing fluid on a dense swarm of particles, Appl. Sci. Res. A1 (1949) 27–34.
[7] K. Nandakumar, J.H. Masliyah, Laminar flow past a permeable sphere, Can. J. Chem. Eng. 60 (1982) 202–211.
[8] R.C. Givler, S.A. Altobelli, A determination of the effective viscosity for the Brinkman–Forchheimer flow model, J. Fluid. Mech. 258 (1994) 355–370.

[9] S. Whitaker, The equations of motion in porous media, Chem. Eng. Sci. 21 (1966) 291–300.
[10] J.C. Slattery, Single-phase flow through porous media, AIChE J. 15 (1969) 866–872.
[11] J. Bear, Dynamics of Fluids in Porous Media, Dover, New York, 1972.
[12] S. Liu, J.H. Masliyah, Single fluid flow in porous media, Chem. Eng. Commun. 148–150 (1996b) 653–732.
[13] P.C. Carman, Fluid flow through granular beds, Trans. Inst. Chem. Eng. 15 (1937) 150–166.
[14] K.E.B. Andersson, Pressure drop in ideal fluidization, Chem. Eng. Sci. 15 (1961) 276–297.
[15] P.K. Agarwal, B.K. O'Neil, Transport phenomena in multi-particle systems – I. Pressure drop and friction factors: unifying the hydraulic-radius and submerged-object approaches, Chem. Eng. Sci. 43 (1988) 2487–2499.
[16] J. Bear, Y. Bachmat, Introduction to Modeling of Transport Phenomena in Porous Media, Kluwer Academic Publishers, 1990.
[17] J.P. Du Plessis, High Reynolds number flow through granular porous media, in: T.F. Russel, R.E. Ewing, C.A. Brebbia, W.G. Gray, G.F. Pinder (Eds.), Computational Methods in Water Resources IX, vol. 2: Mathematical Modelling in Water Resources, Computational Mechanics Publications, Boston, 1992.
[18] S. Liu, Particle dispersion for suspension flow, Chem. Eng. Sci., 1998, submitted for publication.
[19] S. Liu, J.H. Masliyah, On non-Newtonian fluid flow in ducts and porous media, Chem. Eng. Sci. 53 (1998) 1175–1201.
[20] S. Liu, A. Afacan, J.H. Masliyah, A new pressure drop model for flow through orifice plates, 1998, to be submitted for publication.
[21] A. Dybbs, R.V. Edwards, A new look at porous media fluid mechanics – Darcy to turbulent, in: J. Bear, M.Y. Corapcioglu (Eds.), Fundamentals of Transport Phenomena in Porous Media, Martinus Nijihoff Publishers, 1984.
[22] D. Vortmeyer, J. Schuster, Evaluation of steady flow profiles in rectangular and circular packed beds by a variational method, Chem. Eng. Sci. 38 (1983) 1691–1699.
[23] K. Vafai, Convective flow and heat transfer in variable-porosity media, J. Fluid Mech. 147 (1984) 233–259.
[24] M.L. Hunt, C.L. Tien, Non-Darcian flow, heat and mass transfer in catalytic packed-bed reactors, Chem. Eng. Sci. 45 (1990) 55–63.
[25] S. Liu, J.H. Masliyah, Non-Newtonian flow through porous media, in: M. Rahman, C.A. Brebbia (Eds.), Advances in Fluid Mechanics, vol. 9, Computational Mechanics Publications, Southampton, UK, 1996a, pp. 103–112.
[26] R.H. Bahnen, C.G. Stojanoff, Velocity fluctuations at the walls of a packed bed of spheres for medium Re-numbers, ASME J. Fluids Eng. 109 (1987) 242–247.
[27] R. Kufner, H. Hofmann, Implementation of radial porosity and velocity distribution in a reactor model for heterogeneous catalytic gas phase reactions (Torus-Model), Chem. Eng. Sci. 45 (1990) 2141–2146.
[28] G.E. Mueller, Radial void fraction distribution in randomly packed beds of uniformly sized spheres in cylindrical containers, Powder Technol. 72 (1992) 269–275.
[29] R.F. Benenati, C.W. Brosilow, Void fraction distribution in beds of spheres, AIChE J. 8 (1962) 359–361.
[30] L.H.S. Roblee, R.M. Baird, J.W. Tierney, Radial porosity variations in packed beds, AIChE J. 4 (1958) 460–464.
[31] J. Price, The distribution of fluid velocities for randomly packed beds of spheres, Mech. Chem. Eng. Trans. (1968) 7–14.
[32] A. Helmreich, J. Vorwerk, R. Steger, M. Muller, P.O. Brunn, Non-viscous effects in flow of xanthan gum solutions through a packed bed of spheres, Chem. Eng. J. 59 (1995) 111–119.